

High efficiency photodetectors fabricated by electrostatic layer-by-layer self-assembly of CdTe quantum dots

Chang-Ching Tu^{a)} and Lih Y. Lin

Department of Electrical Engineering, University of Washington, Seattle, Washington 98195-2500, USA

(Received 14 August 2008; accepted 30 September 2008; published online 20 October 2008)

We demonstrate high-performance photodetectors from multilayers of CdTe quantum dots (QDs). The QDs are synthesized and dispersed in aqueous solution with either 2-mercaptoethylamine (positively charged) or thioglycolic acid (negatively charged) as capping stabilizers. By electrostatic attraction, the charged QDs are self-assembled layer by layer on an indium tin oxide substrate modified with (3-aminopropyl)triethoxysilane. This process allows control of active layer thickness by self-assembly, and can in principle be applied to a wide range of substrates. The photodetector exhibits high responsivity (0.18 A/W) under 0.1 V bias due to extremely short capping ligands of QDs, which have high internal quantum efficiency, and the densely packed multilayer structure.

© 2008 American Institute of Physics. [DOI: 10.1063/1.3003883]

Colloidal semiconductor quantum dots (QDs) have been used as photosensitizers in various optoelectronic devices, such as photodetectors¹⁻³ and photovoltaic cells,⁴⁻⁶ due to their size-dependent spectral properties,^{7,8} high quantum efficiency through the three-dimensional confinement and potentially carrier multiplication.^{9,10} As opposed to epitaxially grown QDs, functional devices can be achieved by immobilization of QDs on various substrates. Fabrication techniques have been developed in recent years to realize colloidal QD optoelectronic devices, such as spin-coating colloidal QDs^{1,2} and solution-casting QDs/polymer nanocomposite.^{3,4} Based on such techniques, despite of the high performance of their resulting devices, the coverage of QDs and the film thickness cannot be precisely controlled. In this work, we demonstrate photodetectors that consist of layer-by-layer (LBL) self-assembly of QDs on lithographically patterned substrate. The patterned areas are precovered with a monolayer of charged molecules which serve as traps to capture the QDs by electrostatic bonding. Utilizing a similar electrostatic process, the QDs carrying opposite charges are deposited alternately, forming a multilayer film. By virtue of the LBL self-assembly, the film thickness can be controlled by the number of layers. Such fabrication process can be performed on a variety of substrates once their surfaces are modified with dangling hydroxyl groups, including silicon oxide and flexible substrates.

The length of ligands on the nanoparticle surface is critical to achieving high carrier mobility in the QD thin film. It has been reported that cross-linking (necking) of semiconductor QDs can result in significant increase in film conductivity.^{1,11} Although LBL self-assembly of semiconductor QDs has been investigated,^{12,13} the interlinking between QDs from previous works usually involves long alkyl polyelectrolyte, which acts as an insulator and prohibits efficient electron transport. In this work, we use extremely short ligands, 2-mercaptoethylamine (MA) for positive capping and thioglycolic acid (TGA) for negative capping. The lengths of MA (~0.4 nm) and TGA (~0.3 nm) are short enough such that adjacent QDs' surfaces almost contact each other. Since high responsivity is associated with long carrier

recombination time and short carrier transit time, the extremely short ligands used in this work contribute significantly to high responsivity of the photodetectors.

The synthesis of CdTe QDs in aqueous solution using cadmium perchlorate hydrate and Al₂Te₃ was previously reported by Gaponik *et al.*¹⁴ TGA and MA are used as negative and positive thiol stabilizers, respectively, in this work. The precursors are formed in the ratio of Cd²⁺:Te²⁻:thiol stabilizer=1:0.5:2.4 under appropriate pH conditions (11.5 for TGA and 5.75 for MA), and the concentration of Cd²⁺ is kept at 37.6 mM for all samples. The nanocrystals are grown by refluxing the reaction mixture at 100 °C and the particle size is controlled by refluxing time. In the present work, it is controlled to be 24 h for both positively and negatively charged QDs synthesis. The postsynthesis purification methods are different for TGA- and MA-capped QDs. For TGA-CdTe QDs, the size-selective precipitation procedure¹⁴ is applied. The procedure starts with adding 2-propanol dropwise to the as-prepared TGA-CdTe QDs solution under stirring until the whole solution becomes turbid. Then the solution is taken to centrifugation at 3000 rpm for 3 min, followed by decantation of supernatant. The precipitate is dried in vacuum for 2 h and redispersed in de-ionized water to the original volume. For MA-CdTe QDs, it is difficult to precipitate QDs using nonsolvents (such as alcohols), and the amines are relatively unstable. As a result, instead of precipitation, here we use dialysis membrane (molecular weight cutoff=25 000) to remove the crude solvent from QDs. Finally, the pH value of all purified solutions is adjusted to around 7.0 using HCl or NaOH to obtain the best assembly result.¹⁵

For preparing the substrate, an indium tin oxide (ITO)/aluminosilicate (20 nm/0.7 mm in thickness) chip (1.5 cm at each side) is taken to optical lithography using AZ1512 positive photoresist and ITO etchant, forming a 100 μm trench between two electrically separated ITO substrates, as shown in Fig. 1(a). Then the chip is treated with oxygen plasma at 140 mbar and 40 W for 8 min and dipped into 0.05M NaOH for 5 min to increase the density of hydroxide on the ITO surface. Subsequently, the chip is immersed in (3-aminopropyl)triethoxysilane (APTES) solution (1 ml APTES in 20 ml toluene) at 80 °C for 80 h, followed by protonating the amines in diluted HCl solution for few seconds. Upon

^{a)} Author to whom correspondence should be addressed. Electronic mail: tucc@u.washington.edu.

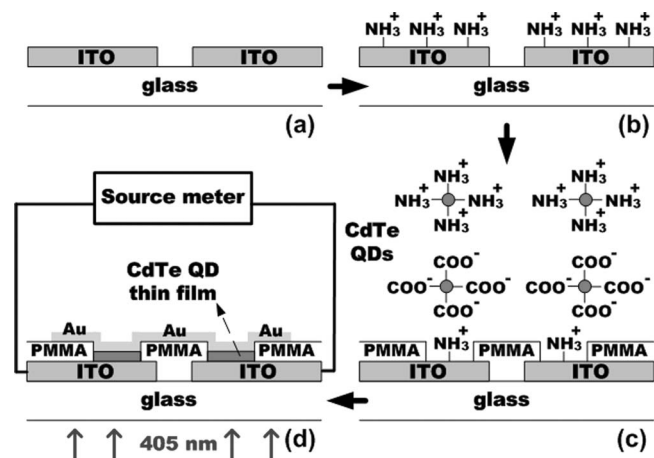


FIG. 1. The overall fabrication process. (a) Two ITO substrates electrically separated by a $100\ \mu\text{m}$ gap. (b) APTES modification on the ITO substrates. (c) After e-beam lithography, two $100\times 100\ \mu\text{m}^2$ PMMA windows are opened on each ITO substrates, on which the LBL self-assembly of CdTe QDs is performed. (d) A thin layer of Au is evaporated on the QD thin film to form the top electrode, while the ITO serves as the bottom electrode.

this step, there is a high area density of positively charged amines (more than $4.8\ \text{NH}_3^+/\text{nm}^2$) (Ref. 16) on the ITO surface, as shown in Fig. 1(b).

Using electron beam (e-beam) lithography and poly(methyl methacrylate) (PMMA) of 90 nm thickness as insulating layer, we are able to define the region for self-assembly, as shown in Fig. 1(c). In this work, two $100\times 100\ \mu\text{m}^2$ PMMA windows are opened on each side of the ITO substrates. The self-assembly of CdTe QDs is performed by immersing the chip into either TGA (negative)- or MA (positive)-CdTe QDs solutions for an hour alternately. After washing away excess QDs with de-ionized water, each time of self-assembly will result in deposition of a monolayer of CdTe QDs. Repeating this process leads to a thin film of multilayer CdTe QDs. Finally, a layer of Au with thickness 100 nm is thermally evaporated on the top as the top electrode, while the ITO substrate serving as the bottom electrode. The final device structure is illustrated in Fig. 1(d).

The absorption and photoluminescence (PL) spectra of CdTe QDs in aqueous solution were obtained with HP 8452A UV-visible spectrometer and Perkin Elmer LS-50B fluorimeter, respectively. The results for MA- and TGA-CdTe QDs are shown in Fig. 2(a). Due to the different natures of ligands, MA-CdTe QDs grow faster than TGA-CdTe QDs, resulting in larger particle size and longer wavelength of emission peak. The exact particle size for both QDs is confirmed by using a FEI Tecnai F20 high-resolution transmission electron microscope (TEM). The imaging results reveal a particle size $\sim 3.5\ \text{nm}$ for MA-CdTe QDs and $\sim 3\ \text{nm}$ for TGA-CdTe QDs, as shown in Fig. 2(b).

The coverage of the LBL self-assembly was characterized by a FEI Sirion scanning electron microscope (SEM). The SEM images of the fabrication result after 7, 14, 21, 30 layers of QD deposition on the ITO substrate are shown in Fig. 3. For the 7- and 14-layer samples, although the assembly of QDs is already uniform throughout the whole substrate, small holes can be observed in the thin film. Through these holes the evaporated Au may penetrate the thin film and connect to the ITO, resulting in a short path between top and bottom electrodes. In our experiment, these shorted devices exhibited very small resistivity, around hundreds of

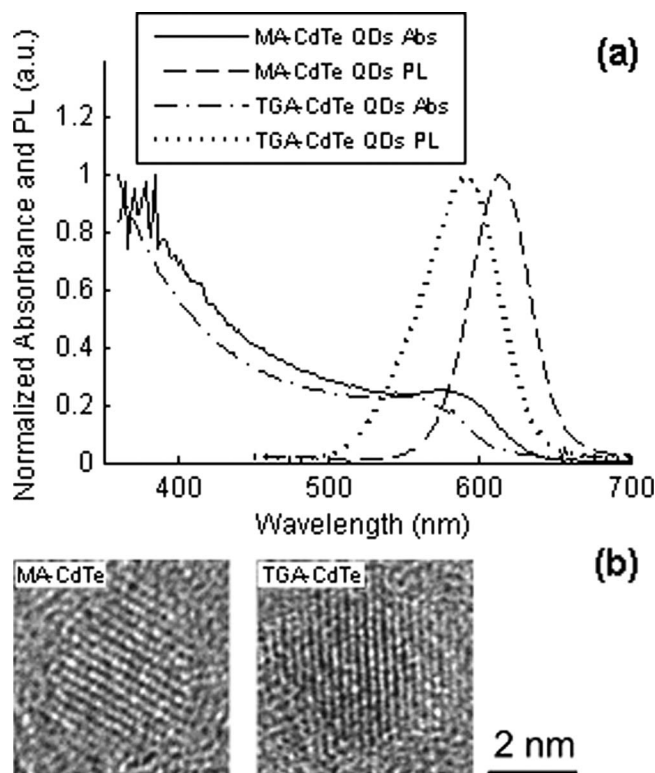


FIG. 2. (a) The UV-visible absorbance and PL spectra of MA- and TGA-CdTe QDs. (b) TEM images of MA- and TGA-CdTe QDs.

Ohms, and no photoconductivity was observed. Therefore, a uniform and thorough coverage of QDs is essential to achieving functional devices. For 21- and 30-layer samples, the coverage of CdTe QDs is very complete while some clusters (30–50 nm in diameter) are formed. Although the QD solution looks clear from macroscale observation after synthesis, small portion of the QDs may aggregate before they are assembled on the substrate. A small cluster in the film grows bigger after each layer of self-assembly process, which results in what we observe in Fig. 3. The average

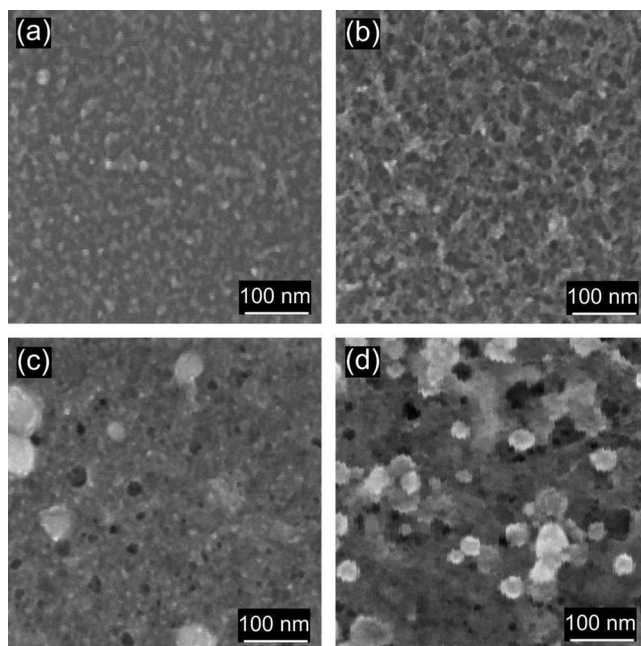


FIG. 3. SEM images of the fabrication result after self-assembly of (a) 7, (b) 14, (c) 21, and (d) 30 layers of CdTe QDs on the ITO substrate.

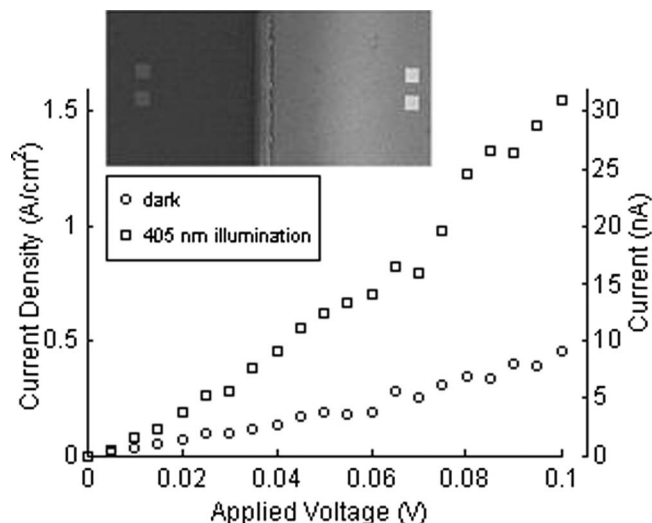


FIG. 4. The measured current and current density of the 30-layer QD photodetector as a function of applied voltages. The inset photograph shows the four PMMA windows of size $100 \times 100 \mu\text{m}^2$ and the $100 \mu\text{m}$ gap that separates the two ITO substrates.

thickness of the 30-layered film is $\sim 120 \text{ nm}$, verified by atomic force microscopy. Based on the ligand length and particle size from TEM characterization, the area density of QDs is estimated to be $1.64 \times 10^6 \text{ QDs}/\mu\text{m}^2$, which corresponds to 1.64×10^{10} QDs in one $100 \times 100 \mu\text{m}^2$ PMMA window.

Photocurrent measurement was performed under ambient environment using a Keithley 6430 subfemtoampere source meter while a Newport LQA 405-40P continuous-wave 405 nm laser, incident from under the glass substrate, was used as the excitation light source. Devices with various numbers of layers were tested. It was found that the 30-layer assembly gives the best and most repeatable result, which we report here. The measured current and current density as a function of applied bias is shown in Fig. 4. The inset SEM micrograph shows the gap ($100 \mu\text{m}$) separating the two ITO substrates and the four square PMMA windows ($100 \times 100 \mu\text{m}^2$) on which the self-assembly is performed. In terms of circuitry model, the device can be represented by two photoconductors in series, each consisting of two windows in parallel. The device generates 22 nA of photocurrent under 0.1 V bias.

The responsivity, defined as the ratio of photocurrent to incident power, is shown in Fig. 5 for voltage bias ranging from 0 to 0.1 V. The power of the 405 nm laser illuminating over the substrate is controlled to be $21.2 \mu\text{W}$ throughout

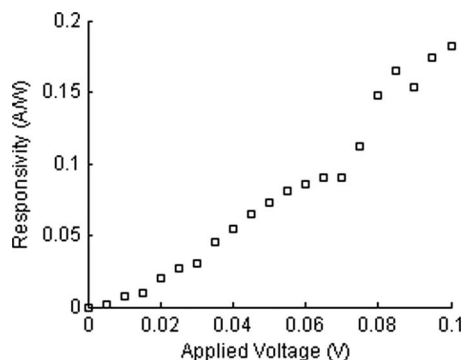


FIG. 5. The measured responsivity of the 30-layer QD photodetector as a function of applied voltages.

the measurement. The laser spot area on the chip is estimated to be $\pi \times (1.5 \text{ mm})^2$, where 1.5 mm is the beam radius at $1/e$ point of the electric field. Therefore, the incident power on the device is estimated to be $21.2 \mu\text{W} \times [4 \times (100 \mu\text{m})^2] / [\pi \times (1.5 \text{ mm})^2] = 0.12 \mu\text{W}$. This corresponds to a responsivity of 0.18 A/W and an external quantum efficiency of 56% at 0.1 V applied bias. The responsivity reported here is higher than the previously reported photodetectors having similar device structures ($\sim 100 \text{ nm}$ in active layer thickness and optical path) under higher bias (up to 5 V) but fabricated by a solution-cast process.³ Through LBL self-assembly of QDs with extremely short ligands, the density of the QDs in the thin film can be maximized, which results in higher absorption volume without compromising carrier transport length. At the same time, the tunneling barriers between adjacent QDs can be significantly reduced. Therefore, higher responsivity can be achieved with the LBL self-assembly structure.

In summary, QD photodetectors have been fabricated by LBL self-assembly of CdTe QDs with extremely short capping ligands. By virtue of the LBL self-assembly, the film thickness can be controlled by the number of layers. The photodetectors reported in this work have high responsivity due to the closely packed layers of QDs obtained through this fabrication process. The position and area for QD deposition can be defined by lithography; therefore, the single-pixel device fabrication can be extended to a planar two-dimensional photodetecting array on a variety of substrates.

This project was supported in part by EBM Technologies. C.-C.T. thanks the University of Washington UIF Graduate Fellowship Program for financial support. We thank Dr. Curtis Chen at the University of Washington for valuable discussions. This work was performed in part at the University of Washington Nanotech User Facility (NTUF), a member of the National Nanotechnology Infrastructure Network (NINN), which is supported by the National Science Foundation.

¹G. Konstantatos, I. Howard, A. Fischer, S. Hoogland, J. Clifford, E. Klem, L. Levina, and E. H. Sargent, *Nature (London)* **442**, 180 (2006).

²G. Konstantatos, J. Clifford, L. Levina, and E. H. Sargent, *Nat. Photonics* **1**, 531 (2007).

³K. R. Choudhury, W. J. Kim, Y. Sahoo, K. S. Lee, and P. N. Prasad, *Appl. Phys. Lett.* **89**, 051109 (2006).

⁴S. A. McDonald, G. Konstantatos, S. Zhang, P. W. Cyr, E. J. D. Klem, L. Levina, and E. H. Sargent, *Nature Mater.* **4**, 138 (2005).

⁵P. V. Kamat, *J. Phys. Chem. C* **111**, 2834 (2007).

⁶W. U. Huynh, J. J. Dittmer, and A. P. Alivisatos, *Science* **295**, 2425 (2002).

⁷A. P. Alivisatos, *Science* **271**, 933 (1996).

⁸C. B. Murray, D. J. Norris, and M. G. Bawendi, *J. Am. Chem. Soc.* **115**, 8706 (1993).

⁹R. D. Schaller, M. Sykora, S. Jeong, and V. I. Klimov, *J. Phys. Chem. B* **110**, 25332 (2006).

¹⁰R. D. Schaller, M. Sykora, J. M. Pietryga, and V. I. Klimov, *Nano Lett.* **6**, 424 (2006).

¹¹D. Yu, C. Wang, and P. Guyot-Sionnest, *Science* **300**, 1277 (2003).

¹²S. Jaffar, K. T. Nam, A. Khademhosseini, J. Xing, R. S. Langer, and A. M. Belcher, *Nano Lett.* **4**, 1421 (2004).

¹³E. Hao and T. Lian, *Langmuir* **16**, 7879 (2000).

¹⁴N. Gaponik, D. V. Talapin, A. L. Rogach, K. Hoppe, E. V. Shevchenko, A. Kornowski, A. Eychmuller, and H. Weller, *J. Phys. Chem. B* **106**, 7177 (2002).

¹⁵H. Hiramatsu and F. E. Osterloh, *Langmuir* **19**, 7003 (2003).

¹⁶C. O. Kim, S. Y. Hong, M. Kim, S. M. Park, and J. W. Park, *J. Clim.* **277**, 499 (2004).